Morphological evolution in single-crystalline Bi$_2$Te$_3$ nanoparticles, nanosheets and nanotubes with different synthesis temperatures

PUNITA SRIVASTAVA and KEDAR SINGH[*]

Department of Physics, Faculty of Science, Banaras Hindu University, Varanasi 221 005, India

Abstract. A general surfactant-assisted wet chemical route has been developed for the synthesis of a variety of bismuth telluride (Bi$_2$Te$_3$) single-crystalline nanostructures with varied morphologies at different temperatures in which hydrazine hydrate plays as an important solvent. Bi$_2$Te$_3$ sheet grown nanoparticles, nanosheets and nanotubes have been synthesized by a simplest wet chemical route at 50, 70 and 100 °C within 4 h. Bi$_2$Te$_3$ sheet grown nanoparticles are obtained in agglomerate state and they are found with many wrinkles. Various types of Bi$_2$Te$_3$ nanotubes are also found which are tapered with one end open and the other closed. X-ray diffraction (XRD), transmission electron microscopy (TEM), selected area electron diffraction (SAED) pattern and energy dispersive X-ray (EDX) spectroscopy were employed to characterize the powder product. It is found that all nanoparticles, nanosheets and nanotubes are well-crystallized nanocrystals and morphologies of the powder products are greatly affected by different synthesis temperatures. The formation mechanisms of bismuth telluride nanostructures are also discussed.

Keywords. Thermoelectric nanostructures; morphological change; chemical synthesis.

1. Introduction

During the past few decades, with rapid enlargement of human society, consumption of traditional energy has increased exponentially. Therefore, more and more researchers came to pay close attention to new sources of energy. Thermoelectric (TE) device emerges as a new kind of hot substance that can directly achieve the conversion between heat and electricity, which can maximize the use of waste heat and electricity in daily life. Thermoelectric (TE) materials can convert waste heat energy to useful electrical energy for power generation which is very important in the present and future life. Decreasing the temperature for refrigeration due to Seebeck and Peltier effects, respectively are expected to play an increasingly imperative role for solving the energy crisis in the future. Bismuth telluride and its alloys are recently known as best TE materials for solid-state cooling devices at room temperature (Boyer and Cissé 1992). However, the real efficiency is still restricted by TE properties available. The energy conversion efficiency mainly depends on the material's dimensionless thermoelectric figure-of-merit (ZT) $= \sigma S^2 T/\kappa$, where σ is the electrical conductivity, S the Seebeck coefficient, T the operating temperature and κ the thermal conductivity. The quantity $S^2\sigma$ is commonly considered as 'power factor'. The wide applications of TE materials have been restrained by the low energy conversion efficiency. So, how to significantly enhance ZT is a crucial factor for wide applications of TE materials. Reducing the dimensionality and size of the building blocks of TE

materials is an efficient and promising way to improve ZT, which has been demonstrated by both theoretical calculations and experimental investigations (Hicks and Dresselhaus 1993a, b; Venkatasubramanian *et al* 2001; Cao *et al* 2008a; Poudel *et al* 2008). In order to be compare competitively with conventional refrigerators and generators, materials having higher ZT larger than 3 are strongly expected. Both theoretical predictions (Hicks and Dresselhaus 1993a, b) and experimental exploration (Dresselhaus *et al* 1999) suggest that nanostructures, quantum wells, quantum wires and quantum dots should have much higher thermoelectric performance than the bulk materials. The highest ZT value of 2·4 has been obtained in Bi$_2$Te$_3$/Sb$_2$Te$_3$ superlattices (Venkatasubramanian *et al* 2001). Even more exciting are the theoretical predictions for one-dimensional nanostructures including nanowires and nanotubes, which are thought to have ZT exceeding 5 (Lin *et al* 2000). For example, one-dimensional (1-D) quantum rods or 2-D quantum wells of Bi$_2$Te$_3$ with a diameter or well width of 5 Å may attain ZT $=$ 14 or 5 by theoretical calculations (Hicks and Dresselhaus 1993a, b) and ZT values of 2·4, 1·47 and 1·4 have been attained from Bi$_2$Te$_3$/Sb$_2$Te$_3$ nanolayer superlattices films at room temperature (Venkatasubramanian *et al* 2001), Bi$_2$Te$_3$/Sb$_2$Te$_3$ bulk nanocomposites at 450 K (Cao *et al* 2008a, b) and nanostructured bismuth antimony telluride bulk alloys at 373 K (Poudel *et al* 2008), respectively. However, if the diameter is >5 nm, electrical transport properties of the nanorods come close to the bulk properties. Bi$_2$Te$_3$ nanostructures with various morphologies such as nanoparticles (NPs) (Jiang and Zhu 2007; Cao *et al* 2008a, b), nanosheets (Shi *et al* 2008), nanowires (Yu *et al* 2004); hollow nanospheres (Jiang *et al* 2007) and nanotubes

[*]Author for correspondence (kedarbhp@rediffmail.com)

(Zhao *et al* 2005; Xiao *et al* 2007; Yao *et al* 2009) have been prepared by various ways, such as solvothermal or hydrothermal methods, electrodepositing, microwave-assisted method and so on. However, solvothermal or hydrothermal reaction processes usually requires high pressure. While electrodepositing method requires expensive template with special construction, on which the product structure strongly depends, while microwave-assisted route is expensive and to be handled carefully. Thus, for a special purpose to develop a more convenient and rapid way for synthesizing Bi_2Te_3 nanostructures is sorely required. During the past decade, low-cost and less hazardous wet-chemical method has been used to synthesize some nanostructures, such as films, nanorods, nanowires and nanobelts of oxides, metals, semimetals, alloys and other compounds (Chen and Ding 2002; Mo *et al* 2002; Peng *et al* 2002; Qiao and Xi 2002). Nowadays, there has been a lot of work on the synthesis of thermoelectric material nanostructures. Previously, a group synthesized skutterudite nanowires for thermoelectric applications (Liu *et al* 2001, 2002). The synthesis of Bi_2Te_3 nanowires have already been reported by an electro-deposition method using porous anodic alumina templates (Sander *et al* 2002). Recently, Sb_2Se_3 nanowires and Bi_2Se_3 nanoflakes have been synthesized through a solvothermal reaction (Ding *et al* 2001; Mo *et al* 2002; Qiao and Xi 2002; Wang *et al* 2003). Bi_2Se_3 nanosheets and nanotubes have been prepared through hydrothermal co-reduction method at 150, 180, 200 and 210 °C (Cui *et al* 2004). However, up to now, there has been little work on the synthesis of Bi_2Te_3 nanosheet and nanotube by this inexpensive wet-chemical route.

In this paper, we report the synthesis of Bi_2Te_3 sheet grown nanoparticles, nanosheets and nanotubes via a simple, inexpensive and less hazardous wet-chemical method at different temperatures (50, 70 and 100 °C) in which hydrazine hydrate plays the role of an important solvent. The powder products are well crystallized single nanocrystals.

2. Experimental

In the synthesis process of Bi_2Te_3 nanoparticles, nanosheets and nanotubes, highly pure tellurium (99·999%) and bismuth chloride ($BiCl_3$) (analytical grade) purchased from Alfa were used without extra purification. Ethylene glycol (EG) and analytical grade hydrazine hydrate ($N_2H_4\cdot H_2O$) purchased from Merck, Germany, were used as received. In the synthesis (10 g) bismuth chloride and (5 g) tellurium (in powder form) were taken with deionized water, ethylene glycol and hydrazine hydrate in a volume ratio of 8:3:1, respectively in a 200 mL capacity conical flask. Then the solution was refluxed under vigorous stirring at 50, 70 and 100 °C for 4 h. Finally, the black precipitates were collected and washed with anhydrous ethanol and hot-distilled water by several times, and then dried in a vacuum at 50 °C for 2 h.

X-ray diffraction (XRD) pattern of as synthesized, freshly dried Bi_2Te_3 was recorded by Rigaku Rotoflux rotating a node diffractometer (operating at 40 kV, 100 mA) with CuKα radiation (wavelength, 1·54 Å). Transmission electron microscopy (TEM) and selected area electron diffraction (SAED) investigations were carried out using Tecnai 20G^2-TEM, employing 200 kV typical e-beam voltage and energy dispersive analysis by X-ray (EDX) using JEOL-JSM-5600.

3. Results and discussion

Figure 1(a–c) shows XRD patterns of the powder products obtained at 50, 70 and 100 °C for 4 h, respectively. All the diffraction peaks in the patterns of all the powder products correspond to the peaks of rhombohedral Bi_2Te_3 (JCPDS no. 08-0021) with space group: $R3m$ (166). The cell parameters in JCPDs no. 08-0021, $a = 4\cdot384$ Å and $c = 30\cdot45$ Å. Therefore, the obtained powder product is rhombohedral Bi_2Te_3.

Figure 2(a,b) shows TEM images of the product sample synthesized at 50 °C for 4 h. Bi_2Te_3 nanoparticles are agglomerated in the diameter range of 25–30 nm. Among these nanoparticles, some ragged or thin or transparent nanosheets are also observed at the surface of these NPs. It is observed that these agglomerate NPs cannot be distinguished from these grown nanosheets. Figure 3(a–c) shows TEM images of the powder product synthesized at 70 °C for 4 h. It is observed that the products are rag-shaped or rolled and thin nanosheets. The corresponding electron diffraction (ED) pattern is shown in figure 3(d). It shows a rhombohedral symmetrical dotted pattern which implies that these nanosheets are well-crystallized single nanocrystals.

Figure 4(a,b) shows TEM images of the product sample synthesized at 100 °C for 4 h. From this figure, it can be seen that some nanotubes are bunched or overlapped together and some are arranged in a separate manner. It is observed that there are some nanotubes in the product with 50–100 nm in diameter, 0·5–1 μm in length and 15–20 nm in wall
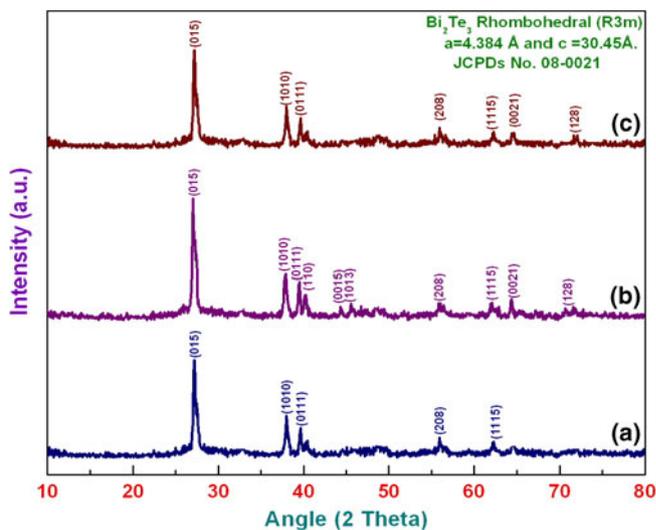

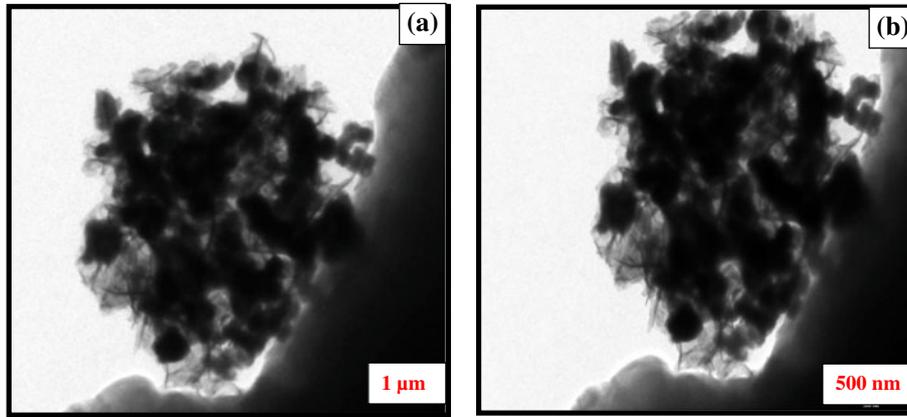**Figure 1.** XRD patterns of powder products synthesized at (**a**) 50, (**b**) 70 and (**c**) 100 °C.

Figure 2. (**a**,**b**) TEM images of Bi$_2$Te$_3$ synthesized at 50 °C.
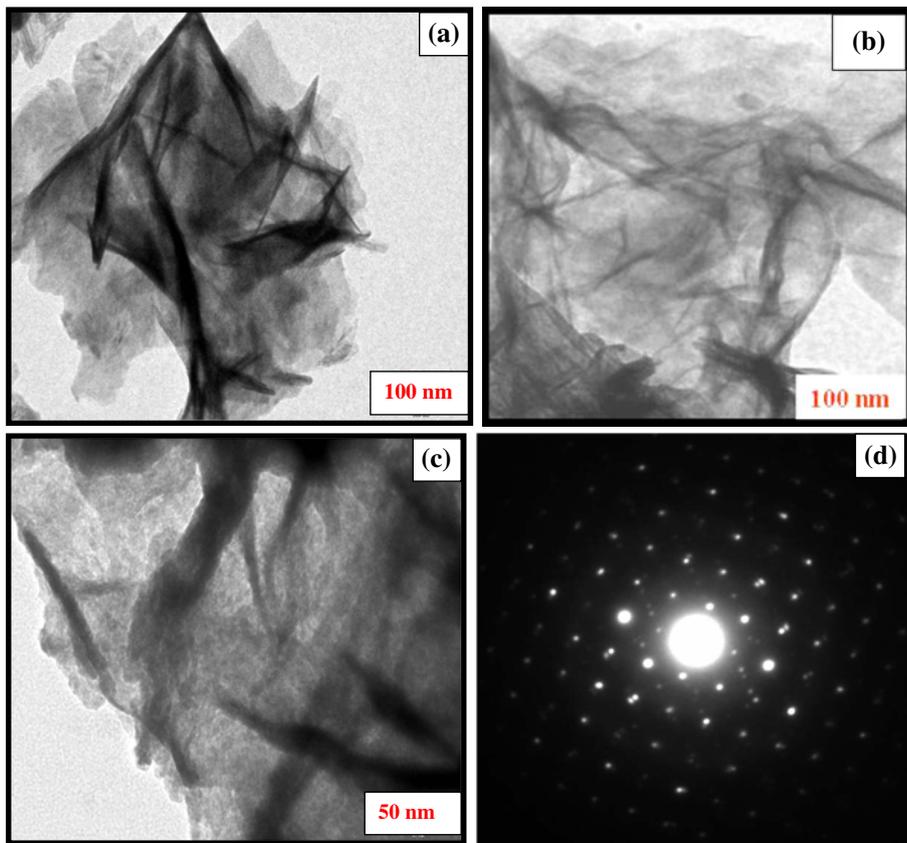

Figure 3. (**a**–**c**) TEM images and (**d**) SAED pattern of synthesized Bi$_2$Te$_3$ nanosheets.

thickness. Figure 4(b) shows typical image of a nanotube, which is tapered with one end open and the other end closed. At the top of the tube, opening of the tube can be seen clearly.

Figure 4(c) shows selected area electron diffraction (SAED) pattern of the nanotube. It indicates a rhombohedral symmetrical dotted pattern implying that the nanotube is well-crystallized single nanocrystals. Figure 5 shows energy dispersive X-ray (EDX) spectroscopy of as-synthesized Bi$_2$Te$_3$ nanostructures. EDX spectroscopy shows that compositional ratio of atoms of Bi/Te is about 2:3 which

is approximately related to the stoichiometric composition of Bi$_2$Te$_3$.

From the above observation, it was found that the morphology of Bi$_2$Te$_3$ sheet grown nanoparticles is highly dependent on used synthesis temperatures. At low temperature (50 °C), some sheets have grown at the surface of nanoparticles. With increasing synthesis temperature (70 °C), only nanosheets are produced with wrinkles and finally at the high temperature (100 °C), the nanosheets got rolled and formed nanotubes.
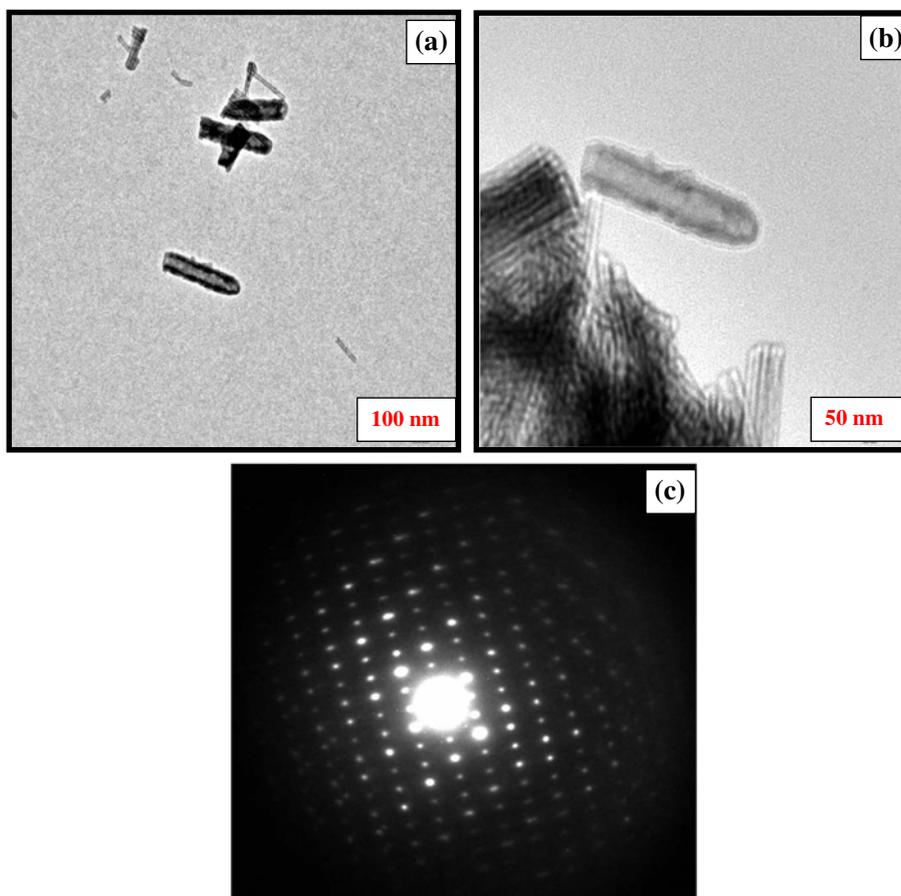
Figure 4. (**a**,**b**) TEM images and (**c**) SAED pattern of synthesized Bi_2Te_3 nanotubes.
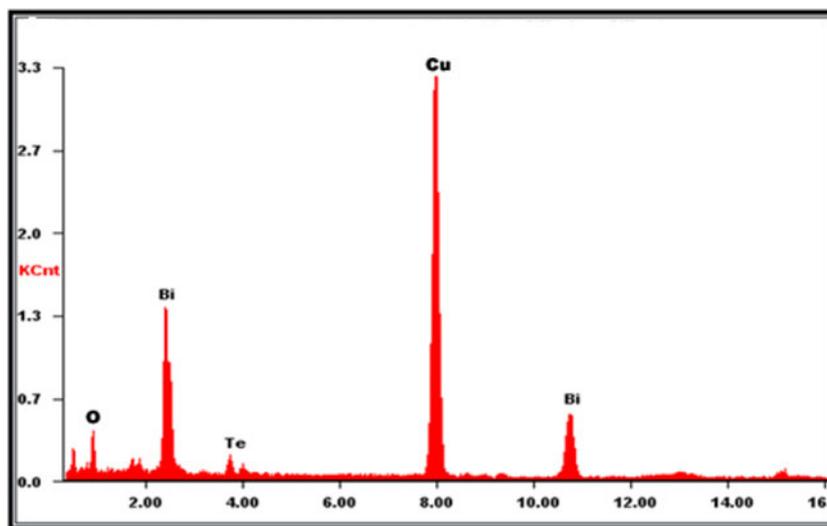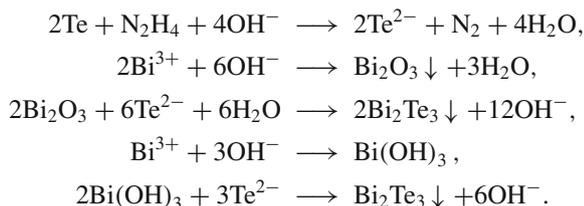

Figure 5. Energy dispersive X-ray spectroscopy of as-synthesized Bi_2Te_3.

Bi_2Te_3 hollow nanospheres have been synthesized through the microwave-assisted route at 150 °C (Jiang *et al* 2007). Bi_2Te_3 nanosheets and nanotubes have been synthesized through the same technique but at higher temperatures (180, 190 and 195 °C) (Yao *et al* 2009).

To further clarify the reaction mechanism involved in the formation of Bi_2Te_3 which is still unclear, it can be reasonably concluded that the suitable ratio of solvents volume may play the critical role for the formation of Bi_2Te_3 nanostructures. On the basis of the above observations, a

growth mechanism of Bi_2Te_3 nanostructures is proposed. In the present work, Te was derived from the reduction of Te by hydrazine hydrate ($N_2H_4 \cdot H_2O$) and highly reactive Te can be easily converted into Te^{2-}. In the initial step, we can recognize the creation of Bi^{3+} and avoid the precipitation of $Bi_2(TeO_3)_3$ and thus provides a more consistent solution environment for the reaction. The chemical reaction involved in the entire synthesis of Bi_2Te_3 nanostructures could be formulated by the following reactions:

$$2Te + N_2H_4 + 4OH^- \longrightarrow 2Te^{2-} + N_2 + 4H_2O,$$
$$2Bi^{3+} + 6OH^- \longrightarrow Bi_2O_3 \downarrow +3H_2O,$$
$$2Bi_2O_3 + 6Te^{2-} + 6H_2O \longrightarrow 2Bi_2Te_3 \downarrow +12OH^-,$$
$$Bi^{3+} + 3OH^- \longrightarrow Bi(OH)_3,$$
$$2Bi(OH)_3 + 3Te^{2-} \longrightarrow Bi_2Te_3 \downarrow +6OH^-.$$

So, the decomposition of precursor can proceed thoroughly under present condition. The application of $N_2H_4 \cdot H_2O$ as the coordination agent is determinable for the phase of the products. So, it can be drawn that the complexing ability of groups containing atom N (such as NH_2 or NH_3) can effectively determine final phase of the products. Compared with the Bi_2O_3 deposit, it is easier for $Bi(OH)_3$ to release Bi^{3+}, which can facilitate growth of nanostructures under non-equilibrium kinetic growth conditions with a high monomer concentration. A similar phenomenon was found during the preparation of Sb_2Te_3 (Srivastava and Singh 2012) and PbSe (Wang *et al* 2008) nanostructures using $N_2H_4 \cdot H_2O$ as complexing agent and the exact mechanism was fully understood.

Based on the above reaction mechanism, it is easy to understand Te was reduced to Te^{2-} and thus, no Te acted as a template. Previously, reports proposed that Te played a role of template to generate telluride in the reactions between elemental Te and non-elemental reactants, for example, Bi_2Te_3 (Zhou *et al* 2006; Chai *et al* 2009), PbTe (Tai *et al* 2008a, b; Liang *et al* 2009), CdTe (Liang *et al* 2009), CoTe (Peng *et al* 2003; Fan *et al* 2008), NiTe (Peng *et al* 2003) and Ag_2Te (Zuo *et al* 2008). All the above results reveal that $N_2H_4 \cdot H_2O$ plays the role of an important solvent in the formation of Bi_2Te_3 nanostructures.

In our research work, we obtained Bi_2Te_3 sheet grown nanoparticles, nanosheet and nanotube through wet chemical route at different synthesis temperatures (50, 70 and 100 °C), but synthesis temperature is much lower than Jiang's and Yao's experiments. The particles morphology and dimension synthesized at low temperatures are completely different from the products prepared at high temperatures (150, 180, 190 and 195 °C). The different morphologies at different synthesis temperatures may be accepted due to the different reaction mechanisms and different adopted methods. So, we can say that wet chemical route is easier and cheap method to synthesize nanosheets and nanotubes at comparatively low temperatures.

Since the investigation of carbon nanotubes, various inorganic nanotubes with layered structure metal have been synthesized by different methods. Bi_2Te_3 also has layered structure with Van der Waals bonds between the neighbouring Te layers, which is equivalent to graphite. The formation of Bi_2Te_3 nanotube also can be described by its layered structure.

The crystal structure of Bi_2Te_3 consists of Bi and Te layers (Nakajima 1963). Bi layer is made up of Bi atoms arranged to form a rhombohedral plane structure and so as a Te layer. It can be explained that each unit cell is packed with two Bi layers and three Te layers by two different types of Te layers, Te(1) and Te(2) are in the following pattern: Te(1)–Bi–Te(2)–Bi–Te(1). The bonding within Te(1)–Bi–Te(2)–Bi–Te(1) layer is considered as covalent, while the bonding between Te(1) and Te(1) layers is Van der Waals forces. Therefore, the crystal cleaves easily between Te(1) planes. The intrinsic crystal properties dominate the nature of primary Bi_2Te_3 particles and it is easier to explain nano-sized single-crystalline sheets, so, the observed nanosheets can be found in the products. When low synthesis temperature is used, growth rate of the crystal is also low. Then, the nanosheets will grow to irregular nanosheets. When the synthesis temperature is increased, the growth rate of Bi_2Te in the reactants solution apparently increases. Because the system will be in a high-energy state, more and more defects will be formed in the structure during the growth process, which will cause the bending or twisting of the nanosheets. With increasing synthesis temperature, edges of the bended or twisted nanosheets will come together. Then the coalesced edges are smoothened out through surface atom diffusion causing large curvature difference between edges and sheet surfaces. To outward appearance, a three-dimensional closed shell with the lowest surface energy, the shell must be curved, which could form Bi_2Te_3 nanotube. Similar phenomenon was also reported previously in the synthesis of metal dichalcogenides nanotubes and nanowires (Yu *et al* 2004; Tenne 2006; Yao *et al* 2009). It was proposed that the high thermal energy induces structural fluctuations in the lamella, leading to folding of the planar nanosheet into a crystalline nanotubular structure. At low temperature, the thermal energy is not sufficiently large to provoke the growth of ultimately more stable nanotubular structure, so only sheets grown nanoparticles appear.

4. Conclusions

Bi_2Te_3 sheets grown nanoparticles, nanosheets and nanotubes have been rapidly synthesized through a wet chemical route at 50, 70 and 100 °C, respectively. XRD measurement proves that the nanocrystals are rhombohedral Bi_2Te_3 with lattice parameters $a = 4 \cdot 384$ Å and $c = 30 \cdot 45$ Å and this rhombohedral structure matches with the corresponding ED pattern. TEM images indicate that the nanoparticles are obtained in the diameter range 25–30 nm with some ragged and thin layers on its surface. Bi_2Te_3 compound is obtained from the compound reaction of bismuth and tellurium from the reaction of Bi^{3+} and Te^{2-} in which $N_2H_4 \cdot H_2O$ plays the

role of an important solvent. Bi_2Te_3 nanotubes grow from bending nuclei. Some nanotubes have been found bunched together and separate also in the product sample synthesized at higher temperatures. From EDX observations, compositional ratio of atoms of Bi/Te is about 2:3, which is approximately related to the stoichiometric composition of Bi_2Te_3.

Acknowledgements

References

Boyer A and Cissé E 1992 *Mater. Sci. Eng.* **B13** 103

Cao Y Q, Zhao X B, Zhu T J, Zhang X B and Tu J P 2008a *Appl. Phys. Lett.* **92** 143106

Cao Y Q, Zhu T J, Zhao X B, Zhang X B and Tu J P 2008b *Appl. Phys.* **A93** 321

Chai Z L, Peng Z P, Wang C and Zhang H J 2009 *Mater. Chem. Phys.* **113** 664

Chen Y T and Ding J B 2002 *Mater. Chem. Phys.* **77** 734

Cui H, Liu H, Li X, Wang J, Han F, Zhang X and Boughton R I 2004 *J. Solid State Chem.* **177** 4001

Ding Z, Viculis L, Nakawatase J and Kaner R B 2001 *Adv. Mater.* **13** 797

Dresselhaus M S, Dresselhaus G, Sun X, Zhang Z, Cronin S B and Koga T 1999 *Phys. Solid State* **41** 679

Fan H, Zhang Y G, Zhang M F, Wang X Y and Qian Y T 2008 *Cryst. Growth Des.* **8** 2838

Hicks L D and Dresselhaus M S 1993a *Phys. Rev. B: Condens. Matter* **47** 16631

Hicks L D and Dresselhaus M S 1993b *Phys. Rev.* **B47** 12727

Jiang Y and Zhu Y J 2007 *J. Crystal Growth* **306** 351

Jiang Y, Zhu Y J and Chen L D 2007 *Chem. Lett.* **36** 382

Liang H W, Liu S, Wu Q S and Yu S H 2009 *Inorg. Chem.* **48** 4927

Lin Y M, Sun X Z and Dresselhaus M S 2000 *Phys. Rev.* **B62** 4610

Liu H, Wang J Y, Hu X B, Gu F, Hua L, Zhang C Q and Teng B 2001 *Chem. Mater.* **13** 151

Liu H, Wang J, Hu X, Li L, Gu F, Zhao S, Gu M, Boughton R I and Minhua J 2002 *J. Alloys Compd.* **334** 313

Mo M, Zeng J, Liu X, Yu W, Zhang S and Qian Y 2002 *Adv. Mater.* **14** 1658

Nakajima S 1963 *J. Phys. Chem. Solids* **24** 479

Peng Q, Dong Y, Deng Z and Li Y 2002 *Inorg. Chem.* **41** 5249

Peng Q, Dong Y J and Li Y D 2003 *Inorg. Chem.* **42** 2174

Poudel B *et al* 2008 *Science* **320** 634

Qiao Z P and Xi G 2002 *J. Solid State Chem.* **166** 49

Sander M S, Prieto A L, Kou H Z, Sands T and Stacy A M 2002 *Adv. Mater.* **14** 665

Shi W D, Zhou L, Song S Y, Yang J H and Zhang H J 2008 *Adv. Mater.* **20** 1892

Srivastava P and Singh K 2012 *Mater. Lett.* **75** 42

Tai G A, Guo W L and Zhang Z H 2008a *Cryst. Growth Des.* **8** 2906

Tai G A, Zhou B and Guo W L 2008b *J. Phys. Chem.* **C112** 11314

Tenne R 2006 *J. Mater. Res.* **21** 2726

Venkatasubramanian R, Silvola E, Colpitts T and Quinn B O 2001 *Nature* **413** 597

Wang D, Yu D, Mo M, Liu X and Qian Y 2003 *J. Crystal Growth* **253** 445

Wang X, Xi G, Liu Y and Qian Y 2008 *Cryst. Growth Des.* **8** 1406

Xiao F, Yoo B Y, Lee K H and Myung N V 2007 *J. Am. Chem. Soc.* **129** 10068

Yao Q, Zhu Y, Chen L, Sun Z and Chen X 2009 *J. Alloys Compd.* **481** 91

Yu H, Gibbs P C and Buhro W E 2004 *J. Mater. Chem.* **14** 595

Zhao X B, Ji X H, Zhang Y H, Zhu T J, Tu J P and Zhang X B 2005 *Appl. Phys. Lett.* **86** 062111

Zhou B, Zhao Y, Pu L and Zhu J J 2006 *Mater. Chem. Phys.* **96** 192

Zuo P F, Zhang S Y, Jin B K, Tian Y P and Yang J X 2008 *J. Phys. Chem.* **C112** 14825